PHYSICAL REVIEW D **92,** 026011 (2015)

Chiral symmetry of SYM theory in hyperbolic space at finite temperature

Kazuo Ghoroku,[1,*] Masafumi Ishihara,[2,†] Motoi Tachibana,[3,‡] and Fumihiko Toyoda[4,§]

[1]*Fukuoka Institute of Technology, Wajiro, Higashi-ku Fukuoka 811-0295, Japan*
[2]*WPI-Advanced Institute for Materials Research (WPI-AIMR), Tohoku University, Sendai 980-8577, Japan*
[3]*Department of Physics, Saga University, Saga 840-8502, Japan*
[4]*Faculty of Humanity-Oriented Science and Engineering, Kinki University, Iizuka 820-8555, Japan*

(Received 22 February 2015; published 30 July 2015)

We study a holographic gauge theory living in the AdS_4 space-time at finite temperature. The gravity dual is obtained as a solution of the type IIB superstring theory with two free parameters, which correspond to four-dimensional cosmological constant (λ) and the dark radiation (C) respectively. The theory studied here is in the confining and chiral symmetry broken phase for $\lambda < 0$ and small C. When C is increased, the transition to the deconfinement phase has been observed at a finite value of $C/|\lambda|$. It is shown here that the chiral symmetry is still broken for a finite range of $C/|\lambda|$ in the deconfinement phase. In other words, the chiral phase transition occurs at a larger value of $C/|\lambda|$ than that of the deconfinement transition. So there is a parameter range of a new deconfinement phase with broken chiral symmetry. In order to study the properties of this phase, we performed a holographic analysis for the meson mass spectrum and other quantities in terms of the probe D7 brane. The results are compared with a linear sigma model. Furthermore, the entanglement entropy is examined to search for a sign of the chiral phase transition. Several comments are given for these analyses.

DOI: 10.1103/PhysRevD.92.026011 PACS numbers: 11.25.Tq, 04.62.+v, 11.10.Wx, 12.38.Aw

I. INTRODUCTION

The holographic approach [1–3] is expected to be applicable also to the supersymmetric Yang Mills (SYM) theory in curved space-time as well as in the flat Minkowski space-time. It would be interesting to make clear the properties of SYM theory in the curved space-time and in the cosmologically developing universe. In this direction, some approaches have been extended to the field theory in the Friedmann-Robertson-Walker (FRW)-type space-time [4–6]. In this case, the four-dimensional (4D) cosmological constant (λ) can be introduced as a free parameter in obtaining the five-dimensional (5D) sector of the ten-dimensional (10D) supergravity solution. The dynamical properties of the 4D SYM theory on the boundary are then characterized by the sign of λ. Through the holographic approach, it has been found that the SYM theory is in the confinement (deconfinement) phase for negative (positive) λ [4–6]. This implies that the dynamical properties of the SYM fields are largely influenced by the geometry of the background space-time.

Furthermore, in this approach, one more free parameter (C) can be introduced as an integration constant in the solution of the supergravity. At first, this term has been added as the "dark radiation" to the 5D supergravity solution in the context of the brane world [7,8]. Since it is defined in the 5D space-time, then its meaning in the 4D theory was mysterious. In this context, afterward, it could be interpreted as the projection of the 5D Weyl term [9,10]. On the other hand, from the viewpoint of holography, it has been found for $\lambda = 0$ that C corresponds to the thermal radiation of the SYM fields at a finite temperature [11]; then the system is in the deconfinement phase. Actually, the 5D metric in this case can be rewritten in the AdS_5-Schwarzschild form, where $C(> 0)$ corresponds to the black hole mass in this metric.

It is easy to imagine that the above two parameters, C and the negative λ, compete with each other to realize the opposite phase of the theory, namely the confinement and the deconfinement respectively. In fact, we find a phase transition at the point where these two opposite effects are balanced [11–15]. As a result, the SYM theory is in the deconfinement phase for $b_0 > r_0$. Here the density of dark radiation C and the magnitude of $|\lambda|$ are denoted by using b_0 and r_0, which are shown in the formula (2.5) of the next section. By using these parameters, the phase diagram of the SYM theory in the FRW space-time is obtained as in Fig. 1.

In the deconfinement phase, the temperature T, which is given by the Hawking temperature of the 5D metric, appears. The critical temperature (T_c) of the confinement-deconfinement transition is given as $T_c = 0$, which corresponds to the critical line $r_0 = b_0$ in Fig. 1. In the region $b_0 > r_0$, the temperature monotonically increases with b_0 for fixed r_0.

*gouroku@dontaku.fit.ac.jp
†masafumi@wpi-aimr.tohoku.ac.jp
‡motoi@cc.saga-u.ac.jp
§ftoyoda@fuk.kindai.ac.jp

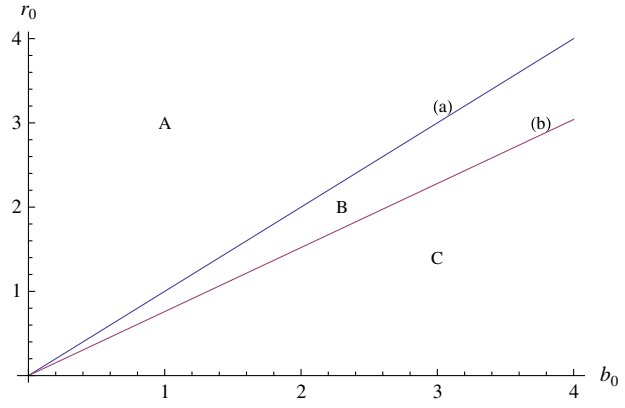

FIG. 1 (color online). The line (a) shows the critical line $r_0 = b_0$ separating the quark-confinement phase (A) and the deconfinement phase (B) and (C). The lower critical line (b) $r_0 = 0.76 b_0$ (χ-br) is separating the chiral symmetry broken phase, (A) and (B), and the symmetry restored phase (C).

It becomes possible to study the properties of the finite temperature SYM theory in the deconfinement phase in the FRW space-time, where the three space is hyperbolic one. As mentioned above, for the case of $\lambda = 0$ and finite b_0, the bulk solution is reduced to the well-known AdS_5 Schwarzschild. So the SYM theory in its special limit of this background has been studied already; see for example [16]. In this case, the two critical temperatures of confinement-deconfinement (T_c) and the chiral symmetry restoration (T_χ) transitions are the same, namely $T_c = T_\chi = 0$. On the other hand, we show here that the value of T_χ shifts from $T_c = 0$. Namely, we find $0 = T_c < T_\chi$ in the case of finite $\lambda(< 0)$, and then the critical line is given by $b_0 = 0.76 r_0$. It is shown in Fig. 1 in the parameter space of b_0 and r_0. Therefore, there exists a new phase in region B of Fig. 1, where the quark and gluons are not confined but the chiral symmetry is not yet restored.

This implies a nontrivial thermal property of the SYM theory in the FRW space-time for negative λ. In order to show and understand the details of this point, we have examined the embedding of the D7 brane in the background. For the embedded D7 brane, we have examined also the spectrum of the Nambu-Goldstone (NG) boson and a massive meson mode in the region of the newly found deconfinement phase where the chiral symmetry is still broken. Then we compare our results with some theoretical consequences obtained from some typical phenomenological models for the chiral symmetry breaking of QCD in order to make clear the dynamical properties implied by our holographic model.

The outline of this paper is as follows. In the next section, a 5D space-time is given by a solution of supergravity as the dual of SYM theory in the AdS_4 background. In Sec. III, the spontaneous chiral symmetry breaking is studied by embedding the D7 probe brane, and then the spectra of two scalar mesons are examined. Since one of them corresponds to the Nambu-Goldstone boson, then the Gell-Mann-Oakes-Renner (GOR) relation and pion decay constant are also examined. In Sec. IV, the mass relations of the two scalars are discussed in terms of the sigma model. We suggest a modified sigma model that is implied by our holographic analysis. In Sec. V, we search a sign of the chiral transition in the entanglement entropy. We could find a change of the behavior of the entanglement entropy, but it could not lead to the phase transition. The summary and discussions are given in the final section.

II. GRAVITY DUAL

The holographic dual to the large N gauge theory embedded in 4D space-time with dark energy and dark radiation is solved by the gravity on the following form of the metric,

$$ds_{10}^2 = \frac{r^2}{R^2}(-\bar{n}^2 dt^2 + \bar{A}^2 a_0^2(t)\gamma_{ij}(x)dx^i dx^j) + \frac{R^2}{r^2}dr^2 + R^2 d\Omega_5^2, \tag{2.1}$$

where

$$\gamma_{ij}(x) = \delta_{ij}\gamma^2(x), \qquad \gamma(x) = 1\Big/\left(1 + k\frac{\bar{r}^2}{4\bar{r_0}^2}\right), \qquad \bar{r}^2 = \sum_{i=1}^{3}(x^i)^2, \tag{2.2}$$

and $k = \pm 1$, or 0. The arbitrary scale parameter $\bar{r_0}$ of three space is set hereafter as $\bar{r_0} = 1$. The solution is obtained from 10D supergravity of type IIB theory [11–14].

The factors $\bar{A}$ and $\bar{n}$ are obtained by introducing two free parameters as mentioned below. Here, we use the following form of solution,

$$\bar{A} = \left(\left(1 + \left(\frac{r_0}{r}\right)^2\right)^2 + \left(\frac{b_0}{r}\right)^4\right)^{1/2}, \tag{2.3}$$

$$\bar{n} = \frac{(1 + (\frac{r_0}{r})^2)^2 - (\frac{b_0}{r})^4}{\bar{A}}, \tag{2.4}$$

$$r_0 = \sqrt{|\lambda|}R^2/2, \qquad b_0 = R\tilde{c}_0, \qquad \tilde{c}_0 = CR^3/(4a_0^4), \tag{2.5}$$

where the dark radiation C is introduced as an integral constant in solving the equation of motion. This solution expresses the case of negative λ. Here, the dark energy (or cosmological term) $\lambda(t)$ is introduced by the following equation:

$$\left(\frac{\dot{a}_0}{a_0}\right)^2 + \frac{k}{a_0^2} = \lambda. \tag{2.6}$$

Although it is possible to consider a time dependent λ as in [11], we set it here as a constant λ for simplicity. In the following, our discussion concentrates on the case of negative constant λ and we assume small time derivative of $a_0(t)$. We should notice the following fact that the solution $a_0 = 1/\sqrt{|\lambda|} =$ constant is actually allowed for negative constant λ and $k = -1$.

III. CHIRAL PHASE TRANSITION AT FINITE TEMPERATURE

A. D7-brane embedding

We study the chiral condensate and the $q - \bar{q}$ meson spectrum of the boundary theory by embedding the probe D7 brane for the flavor quarks. The D7-brane action is given by the Dirac-Born-Infeld (DBI) and the Chern-Simons terms as follows:

$$\begin{aligned} S_{D7} &= -\tau_7 \int d^8\xi e^{-\Phi}\sqrt{-\det\left(g_{ab} + 2\pi\alpha' F_{ab}\right)} \\ &\quad + T_7 \int \sum_i (e^{2\pi\alpha' F_{(2)}} \wedge c_{(a_1 \ldots a_i)})_{0\ldots 7}, \\ g_{ab} &\equiv \partial_a X^\mu \partial_b X^\nu G_{\mu\nu}, \\ c_{(a_1\ldots a_i)} &\equiv \partial_{a_1} X^{\mu_1} \ldots \partial_{a_i} X^{\mu_i} C_{\mu_1 \ldots \mu_i}, \end{aligned} \tag{3.1}$$

where τ_7 is the brane tension. The DBI action involves the induced metric g_{ab} and the $U(1)$ world volume field strength $F_{(2)} = dA_{(1)}$.

The solution given in the previous section is obtained for the case of constant dilaton. So it does not play any role in the present case. For simplicity, we consider the dual theory on the boundary at $r = \infty$. Then the induced metric for the above D7 brane is obtained as follows. Consider the above background (2.1) and rewrite it as follows:

$$ds_{10}^2 = \frac{r^2}{R^2} ds_{(4)}^2 + \frac{R^2}{r^2} dr^2 + R^2 d\Omega_5^2, \tag{3.2}$$

$$= \frac{r^2}{R^2} ds_{(4)}^2 + \frac{R^2}{r^2}\left(d\rho^2 + \rho^2 d\Omega_3^2 + \sum_{i=8}^{9} dX^{i2}\right), \tag{3.3}$$

where

$$ds_{(4)}^2 = (-\bar{n}^2 dt^2 + \bar{A}^2 a_0^2(t)\gamma_{ij}(x) dx^i dx^j), \tag{3.4}$$

$$r^2 = \rho^2 + (X^8)^2 + (X^9)^2. \tag{3.5}$$

Then the induced metric of the D7 brane is obtained as

$$ds_8^2 = \frac{r^2}{R^2} ds_{(4)}^2 + \frac{R^2}{r^2}((1 + w'^2) d\rho^2 + \rho^2 d\Omega_3^2), \tag{3.6}$$

where the profile of the D7 brane is taken as $(X^8, X^9) = (w(\rho), 0)$ and $w' = \partial_\rho w$; then

$$r^2 = \rho^2 + w^2. \tag{3.7}$$

In the present case, there is no R-R filed, so the action is given as

$$S_{D7} = -\tau_7 \Omega_3 \int d^4x a_0^3(t)\gamma^3(x) \int d\rho \rho^3 \bar{n}\bar{A}^3 \sqrt{1 + w'^2(\rho)}, \tag{3.8}$$

where Ω_3 denotes the volume of S^3 of the D7 brane world volume.

From this action, the equation of motion for w is obtained as

$$\begin{aligned} &w'' + \left(\frac{3}{\rho} + \frac{\rho + w w'}{r}\partial_r(\log(\bar{n}\bar{A}^3))\right) w'(1 + w'^2) \\ &\quad - \frac{w}{r}(1 + w'^2)^2 \partial_r(\log(\bar{n}\bar{A}^3)) = 0. \end{aligned} \tag{3.9}$$

The constant $w \neq 0$ is not the solution of this equation, so the supersymmetry is broken except for the case of trivial solution $w = 0$.

B. Embedded solutions and chiral symmetry breaking

In the confinement region, the chiral symmetry is spontaneously broken as shown in [11]. The phase transition of the present model to the deconfinement occurs when the density of the dark radiation increases and exceeds a critical point, which is given by $b_0 = r_0$ (see Fig. 1). From this point, the Hawking temperature, $T_H (= \frac{\sqrt{2} b_0}{\pi R^2}\sqrt{1 - (r_0/b_0)^2})$, appears for $b_0 > r_0$. At this stage, when the temperature appears, the chiral symmetry is usually restored. In the present case, however, we could observe the chiral symmetry restoration after transferring into the deconfinement phase at a finite T_H, which depends on r_0, as shown in Fig. 1 above. These facts are explained below through the numerical analysis.

All solutions of the above Eq. (3.9) have the following asymptotic form:

$$w(\rho) = m_q + \frac{c + 4 m_q r_0^2 \log(\rho)}{\rho^2} + \cdots \tag{3.10}$$

at large ρ. In the second term of the right-hand side of (3.10), the term proportional to $\log(\rho)$ arises from the loop corrections of the SYM theory since the conformal symmetry would be broken due to the existence of the cosmological constant in the present case [4–6]. We could show however that this term is proportional to the quark mass m_q, which is given by the asymptotic value of $w(\infty)$. In order to see the spontaneous chiral symmetry breaking, it is enough to see chiral condensate $\langle\bar{\Psi}\Psi\rangle = c = \rho^2 w|_{\rho\to\infty}$. Then the analysis is simply performed for $m_q = 0$.

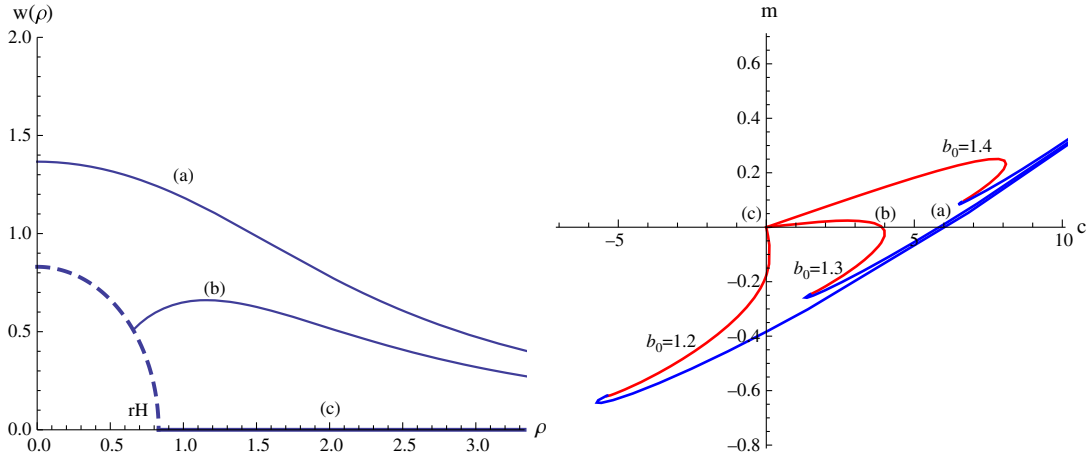

FIG. 2 (color online). Left: The solutions of $w(\rho)$ with $m_q = 0$ for $b_0 = 1.3r_0$, and $r_0 = 1.0$. The solution (c) represents the trivial one, $w = 0$. The dashed curve denotes the horizon $r_H = \sqrt{b_0^2 - r_0^2}(= 0.83)$. Right: The $c - m_q$ relations of embedded solutions for $b_0 = 1.2$, 1.3, and 1.4 are shown with the same other parameters of the left figure. For the case of $b_0 = 1.3$, the embedded solutions at the three points, (a), (b), and (c), are shown in the left figure.

We have therefore examined the numerical solutions for $m_q = 0$ at various points in the parameter space $b_0 - r_0$ in order to find the transition points. Three typical solutions are shown in the left figure of Fig. 2. They are classified as Minkowski type (M type) ($w(0) > r_H = \sqrt{b_0^2 - r_0^2}$), black hole type (B type), which ends on r_H at $\rho = \rho_{\min}$, and the trivial solution $w = 0$, which is always the solution of Eq. (3.9).

We notice that the above M and B types of embedded configuration of D7 brane correspond to the one of connected and disconnected D8 and $\bar{D}8$ branes in the Sakai-Sugimoto model at finite temperature [17].

We performed the numerical analyses for fixed $r_0 = 1$ by varying b_0. In this case, the region of b_0 is separated to the following three one.

(i) For $b_0 > 1.31$, we find only the trivial solution for $m_q = 0$. Then the chiral symmetry is restored.
(ii) For $1.28 < b_0 < 1.31$, there are three types of solution mentioned above.
(iii) For $b_0 < 1.28$, there are M-type and trivial solutions.

The distributions of the general solutions including these three types are shown in the right of Fig. 2 for $b_0 = 1.2$, 1.3, and 1.4. Then one might consider that the chiral symmetry may be broken in the region $b_0 < 1.31$; however, we must compare the free energies in order to see which solution is favored for the given b_0 when plural solutions for the same m_q exist.

The free energy for each solution is obtained by substituting the solution $w(\rho)$ into the Wick rotated Eucledian D7 action (3.8). Here, the normalized free energy,

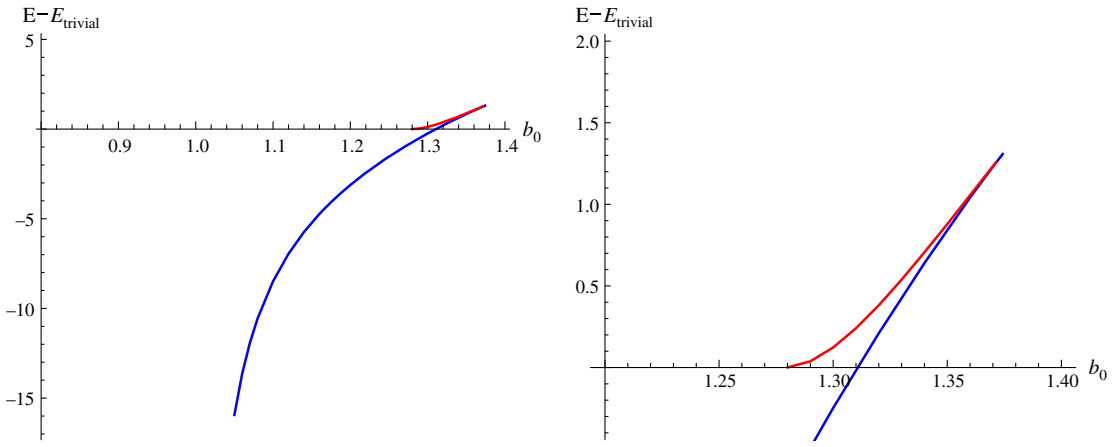

FIG. 3 (color online). Left: The blue (red) curve denotes the free energy difference, $E - E_{\text{trivial}}$, between the one for the Minkowski (black hole) embedding solutions of $w(\rho)$ with $m_q = 0$ and for the trivial solution $w = 0$. Right: The part, where the blue curve crosses zero, of the left-hand figure is enlarged.

$$E = \int d\rho \rho^3 \bar{n}\bar{A}^3 \sqrt{1+w'^2(\rho)}, \tag{3.11}$$

is evaluated, and then the values subtracting the one for the trivial solution are shown in Fig. 3.

This figure shows the following:

(i) The free energy of the B-type solution is always larger than the other two. Thus, this type of solution cannot be realized.

(ii) The value of $E_{M\text{-type}} - E_{\text{trivial}}$ crosses zero at $b_0 = 1.31$. This implies that a transition from the M-type solution ($\langle\bar{\Psi}\Psi\rangle = c > 0$) to the trivial solution ($\langle\bar{\Psi}\Psi\rangle = 0$) occurs at this point. This point is therefore the chiral phase transition point. The order parameter $\langle\bar{\Psi}\Psi\rangle$ has a gap at this transition point.

The transition line $b_0 = 1.31 r_0$ is shown in Fig. 1. As a result, we find two critical lines (a) and (b) in the parameter plane (b_0, r_0). Line (a) represents the transition point from confinement to deconfinement and (b) represents the critical line from the chiral symmetry breaking phase to the restoring phase. This result implies the fact that the density of the dark radiation necessary for the restoration of the chiral symmetry is larger than the one needed for realizing the deconfinement phase.

We recall that the role of the dark radiation is to screen the force needed for the confinement. The same kind of force would be necessary for the spontaneous mass generation of massless quarks. The above result, that the chiral transition needs a larger value of C than the case of the confinement-deconfinement transition, implies that the range of the force necessary to break the chiral symmetry is shorter than the one for the confinement.

IV. CHIRAL PHASE TRANSITION AND THE NG BOSONS

We study the meson spectra by solving the equations of motion for the fluctuation of fields on the D7 brane. In the A phase in Fig. 1, we find the NG bosons and the GOR relation [18] for massless and small mass quarks, respectively. While in the B phase, in spite of the fact that quarks are deconfined, we expect the existence of the NG boson and a massive scalar mode due to spontaneous chiral symmetry breaking.

To compute the meson spectra, let us consider the fluctuations of the scalar fields defined as

$$X^8 = w(\rho) + \tilde{\phi}^8, \qquad X^9 = \tilde{\phi}^9.$$

$\tilde{\phi}^8$ and $\tilde{\phi}^9$ correspond to the NG boson and a massive scalar boson, respectively. Note here that this phenomenon also represents the breaking of a global $U(1)$ symmetry.

The wave functions are given in the following factorized form:

$$\tilde{\phi}^k = \varphi^k(t, x^i)\phi_l^k(\rho)\mathcal{Y}_l(S^3), \qquad (k = 8, 9),$$

where $\mathcal{Y}_l(S^3)$ denotes the spherical harmonic function on a three-dimensional sphere with the angular momentum l.

Then the linearized field equations of $\phi_l^9(\rho)$ and $\phi_l^8(\rho)$ for $w \neq 0$ are given as follows:

$$\partial_\rho^2\phi_l^9 + \frac{1}{L_0}\partial_\rho(L_0)\partial_\rho\phi_l^9 + (1+w'^2) \times \left[\left(\frac{R}{r}\right)^4 \frac{m_9^2}{\bar{n}^2} - \frac{l(l+2)}{\rho^2} - 2K_{(1)}\right]\phi_l^9 = 0, \tag{4.1}$$

$$L_0 = \rho^3\bar{n}\bar{A}^3\frac{1}{\sqrt{1+w'^2}}, \qquad K_{(1)} = \frac{1}{\bar{n}\bar{A}^3}\partial_{r^2}(\bar{n}\bar{A}^3) \tag{4.2}$$

and

$$\partial_\rho^2\phi_l^8 + \frac{1}{L_1}\partial_\rho(L_1)\partial_\rho\phi_l^8 + (1+w'^2) \times \left[\left(\frac{R}{r}\right)^4 \frac{m_8^2}{\bar{n}^2} - \frac{l(l+2)}{\rho^2} - 2(1+w'^2)(K_{(1)} + 2w^2K_{(2)})\right]\phi_l^8 = -2\frac{1}{L_1}\partial_\rho(L_0 w w' K_{(1)})\phi_l^8 \tag{4.3}$$

$$L_1 = \frac{L_0}{1+w'^2}, \qquad K_{(2)} = \frac{1}{\bar{n}\bar{A}^3}\partial_{r^2}^2(\bar{n}\bar{A}^3). \tag{4.4}$$

Here are some remarks.

(i) For the 4D part of the wave function, $\varphi^k(x^\mu)$, we have assumed the following eigenvalue equation:

$$\Box_4\varphi^k(x^\mu) = \frac{1}{\sqrt{\tilde{g}_4}}\partial_\mu\sqrt{\tilde{g}_4}\tilde{g}^{\mu\nu}\partial_\nu\varphi^k(x^\mu) = m_k^2\varphi^k(x^\mu), \tag{4.5}$$

where $\tilde{g}_4 = -\det\tilde{g}_{\mu\nu}$ and

$$\tilde{g}_{\mu\nu}dx^\mu dx^\nu = (-dt^2 + a_0^2(t)\gamma_{ij}(x)dx^i dx^j). \tag{4.6}$$

(ii) The operator $\Box_4$ is derived from the eight-dimensional Laplacian $\Box_8$ for the metric (3.6) induced on the D7 brane. In fact, $\Box_8$ is expanded as

$$\Box_8 = \frac{1}{\sqrt{g_{(8)}}}\partial_a g^{ab}\sqrt{g_{(8)}}\partial_b, = \frac{1}{\sqrt{g_{(8)}}}\partial_\mu g^{\mu\nu}\sqrt{g_{(8)}}\partial_\nu + \cdots, \tag{4.7}$$

$$\sqrt{g_{(8)}} = \sqrt{g_{(4)}}\rho^3\sqrt{1+w'^2}, \qquad \sqrt{g_{(4)}} = (a_0\gamma\bar{A})^3\bar{n}, \tag{4.8}$$

where $a, b = 0$–7, $\mu, \nu = 0$–3 and the elliptics denotes the derivative terms with respect to the other coordinates, ρ and the one of S^3.

By using the above expansion and the approximation to neglect the time derivative of $a_0(t)$, we arrive at the above

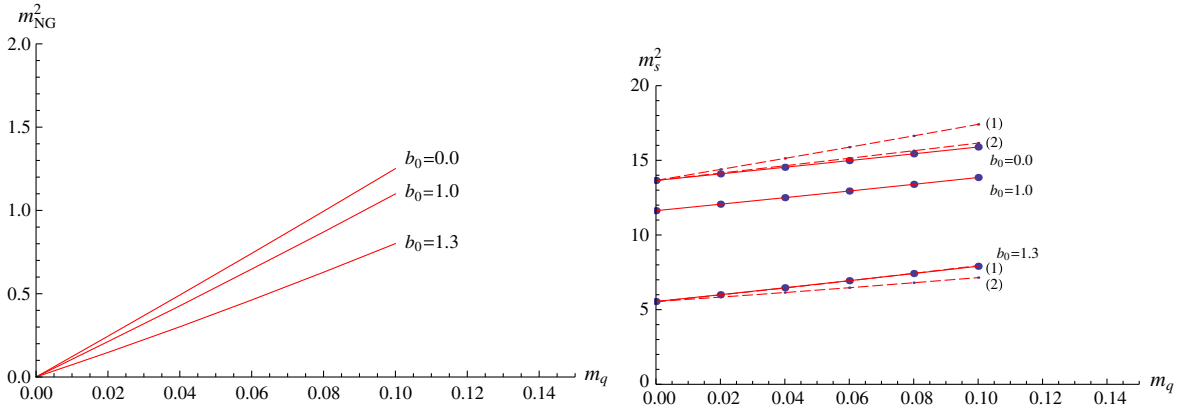

FIG. 4 (color online). Left: The quark mass(m_q) dependence of $m_{\rm NG}^2$ [Nambu-Goldstone boson (ϕ^9)]. Right: The m_s^2 (red line) for massive scalar (ϕ^8) is shown by the solid lines. The dotted lines are the prediction from the sigma model given below. The line (1) denotes the one for (4.12) and (2) for (4.16).

Eqs. (4.1) and (4.3), which are used to find the meson spectra [6].

A. Numerical results

Figure 4 is the numerical result for the quark mass dependence of the mass eigenvalues $m_8(m_s)$ and $m_9(m_{\rm NG})$, which correspond to ϕ^8 (massive scalar) and ϕ^9 (Nambu-Goldstone boson), respectively. From the left panel of Fig. 4, we find the NG boson mass behaves as $m_{\rm NG}^2 \propto m_q$, which is consistent with the GOR relation.

The GOR relation is expressed as

$$m_{\rm NG}^2 = \frac{2m_q\langle\bar{\Psi}\Psi\rangle}{f_\pi^2}, \tag{4.9}$$

where f_π denotes the pion decay constant. Since $\langle\bar{\Psi}\Psi\rangle$ is obtained for various b_0s through the solution of the D7-brane profile, then we can determine the b_0 dependence of f_π through the GOR relation (4.9). Figure 5 shows the numerical results.

Here are our findings. f_π is almost constant within the confinement regime ($b_0 < r_0$), and then it increases with b_0 in the deconfinement regime ($b_0 > r_0$). This result seems to be reasonable since the decay channels may increase in the deconfinement regime.

B. Comparison with the linear σ model

In principle, it would be possible to derive an effective theory of mesons from the D7-brane action as a functional of ϕ^8 and ϕ^9. Then the correspondence of the parameters in the D7-brane action to the one of the sigma model will be obtained. However, there are various possibilities for higher order terms of the meson fields. Then the resultant effective action would get very complicated, which is not useful to analyze.

Instead let us compare the results we obtained in the above with those from the linear sigma model. At the mean field level, the Lagrangian density of the linear sigma model is given by

$$\mathcal{L} = \frac{\mu^2}{2}(\sigma^2+\pi^2) - \frac{\lambda}{4}(\sigma^2+\pi^2)^2 + h\sigma, \tag{4.10}$$

where μ, λ, and h are the parameters while σ and π are the mean fields. The last term proportional to h, which plays a role of the quark mass term, breaks $U(1)$ chiral symmetry

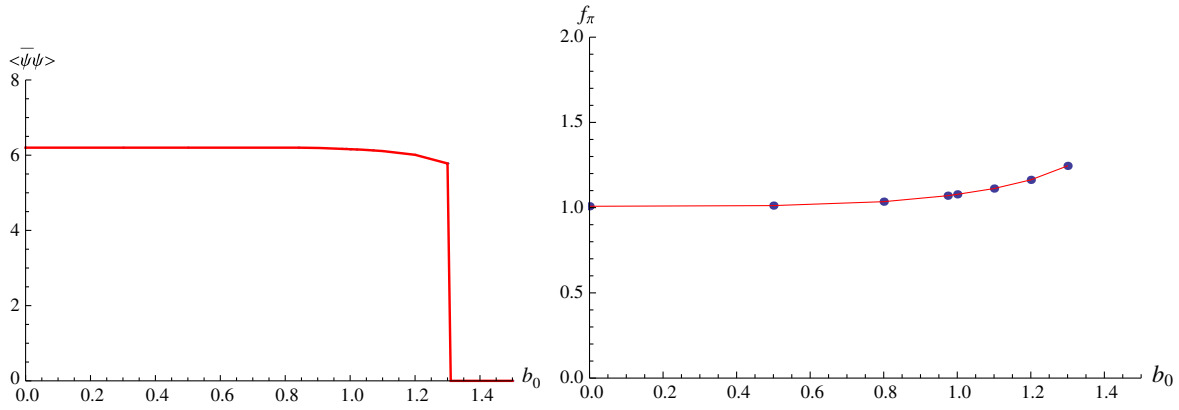

FIG. 5 (color online). b_0 dependence of the chiral condensate $\langle\bar{\Psi}\Psi\rangle$ and the pion decay constant f_π.

explicitly. For the small value of h, the vacuum is determined from the stationary conditions $\frac{\partial \mathcal{L}}{\partial \sigma} = \frac{\partial \mathcal{L}}{\partial \pi} = 0$, which lead us to

$$(\sigma, \pi) = \left(f_\pi + \frac{h}{2\mu^2}, 0 \right) \tag{4.11}$$

with $f_\pi \equiv \sqrt{\frac{\mu^2}{\lambda}}$. Then one obtains the mass spectra such that

$$M_\pi^2(h) = \frac{h}{f_\pi}, \qquad M_\sigma^2(h) = 2\mu^2 + \frac{3h}{f_\pi} = 2\mu^2 + 3M_\pi^2(h). \tag{4.12}$$

In the right panel of Fig. 4, we compared the results (4.12) with those obtained from the holographic method. Note here that the parameter region for b_0 is restricted to the confinement phase ($b_0 < r_0$). Hereafter, we set $r_0 = 1$. The reason why we consider the linear sigma model only for the confinement phase is obvious because the Lagrangian density is solely written in terms of mesons.

The results (4.12) definitely deviates from our holographic ones. It looks to have a rather good fit to the result with $b_0 = 1.3$. So we might modify the sigma model in order to obtain a better fit to our results in the region of $b_0 < 1$.

This is performed by adding the next order term of $(\sigma^2 + \pi^2)$ as follows:

$$\mathcal{L} = \frac{\mu^2}{2}(\sigma^2 + \pi^2) - \frac{\lambda_1}{4}(\sigma^2 + \pi^2)^2 - \frac{\lambda_2}{6}(\sigma^2 + \pi^2)^3 + h\sigma. \tag{4.13}$$

This type of modification is justified as far as it is based on the derivation of the effective sigma model by expanding the D7-brane action in terms of the π and σ fields.

The vacuum is determined as the configuration $(\sigma, \pi) = (\sigma_0, 0)$, which is the real solution of the following equation:

$$h = (-\mu^2 + \lambda_1\sigma_0^2 + \lambda_2\sigma_0^4)\sigma_0. \tag{4.14}$$

Then the meson masses are given as

$$M_\pi^2 = -\mu^2 + \lambda_1\sigma_0^2 + \lambda_2\sigma_0^4 = \frac{h}{\sigma_0},$$
$$M_\sigma^2 = -\mu^2 + 3\lambda_1\sigma_0^2 + 5\lambda_2\sigma_0^4. \tag{4.15}$$

From (4.15), we find

$$M_\sigma^2 = 2M_\pi^2 + \mu^2 \tag{4.16}$$

by setting the following relation among the parameters,

$$\lambda_2 = -\frac{\lambda_1}{3\sigma_0^2}. \tag{4.17}$$

This relation is a sort of tuning to obtain (4.16), which provides a better fit to our holographic results (see the right panel of Fig. 4).

V. ENTANGLEMENT ENTROPY NEAR THE TRANSITION REGION

We study the entanglement entropy ($S_{\rm EE}$) near the transition region to find a signature of the phase transition. $S_{\rm EE}$ is given by calculating the minimum area of the surface A whose boundary ∂A is set at the boundary of the bulk. As given in [19,20] the holographic entanglement entropy is given by

$$S_{\rm EE} = \frac{S_{\rm area}}{4G_N^{(5)}}, \tag{5.1}$$

where $S_{\rm area}$ denotes the minimal surface whose boundary is defined by ∂A and the surface is extended into the bulk.

We see the regularized finite part $\bar{S}_{\rm finite}$. The detailed calculations are given in [14,15]. This quantity contains two contributions from the curvature r_0 and the dark radiation b_0. In order to see how the dark radiation affects the entropy, we consider the following quantity,

$$S_{\rm finite} \equiv \bar{S}_{\rm finite} - \bar{S}_{\rm finite}|_{b_0=0}, \tag{5.2}$$

by subtracting the $\bar{S}_{\rm finite}|_{b_0=0}$ from $\bar{S}_{\rm finite}$.

Figure 6 shows the relation between $S_{\rm finite}/V$ and b_0. V is the volume of the sphere with radius $p = p_0$ in FRW$_4$ space,

$$V = 4\pi a_0^3 \int_0^{p_0} \gamma^3 p^2 dp$$
$$= 2\pi a_0^3 \left(\frac{4p_0(4 + p_0^2)}{(p_0^2 - 4)^2} + \log\frac{2 - p_0}{2 + p_0} \right). \tag{5.3}$$

From the results shown in Fig. 6, we can observe the following.

(i) As shown in Fig. 6, for small b_0 region, $S_{\rm finite}/V$ is small and $S_{\rm finite}/V \propto b_0^4$. The energy density of the dark radiation is also proportional to b_0^4. Thus, the small deviation of $S_{\rm finite}$ and the energy density will lead to the first law of the thermodynamics. On this point, we will discuss more in the near future.

(ii) For large $b_0 > 1$ region, on the other hand, it increases with b_0 rapidly and $S_{\rm finite}/V \propto T_H^3$ where the Hawking temperature $T_H(b_0)$ is given as [15]

$$T_H(b_0) = \frac{\sqrt{2}b_0}{\pi R^2}\sqrt{1 - (r_0/b_0)^2}. \tag{5.4}$$

Thus, at large b_0 region, the entanglement entropy becomes the thermal entropy [21]. This behavior is expected as a high temperature behavior of the entanglement entropy $S_{\rm finite}/V$.

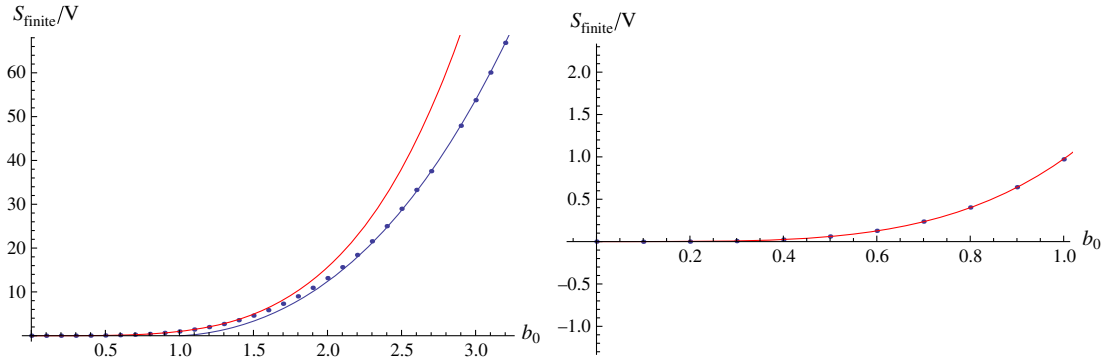

FIG. 6 (color online). The left figure is the relation between S_{finite}/V and b_0 for $r_0 = R = 1$ and $a_0 = 0.5$. For large b_0 region and small b_0 region, S_{finite}/V can be fitted by $S_{\text{finite}}/V = 26.1T_H^3$ (blue line) and $S_{\text{finite}}/V = 0.97b_0^4$ (red line), respectively. The right figure shows the relation at small b_0 region. There is no specific phenomenon at the chiral transition point ($b_0 = 1.31$).

(iii) However, as far as we observe Fig. 6, there is no specific signature at the chiral transition point ($b_0 \sim 1.31$) in the behavior of the entanglement entropy.

VI. SUMMARY AND DISCUSSION

We have studied SYM theory in the AdS_4 space-time. The holographic dual is expressed by a 10D supergravity solution that is described by two free parameters corresponding to the negative 4D cosmological constant and the dark radiation. These two quantities work in opposite directions to realize a typical phase of the theory. The negative λ leads the theory to the confinement phase. However, the dark radiation prevents it. Then we find the confinement-deconfinement transition at their balanced point, $r_0 = b_0$, as shown previously.

Here, we have pointed out that the chiral symmetry restoration does not occur yet at $r_0 = b_0$ as expected in the case of usual QCD. The chiral transition is found at $b_0 = 1.31r_0$ after the deconfinement transition. So there exists a new phase, where chiral symmetry is broken but the quarks and gluons are deconfined. It is shown as region B in the phase diagram in Fig. 1. In this region, the Nambu-Goldstone boson is certainly observed, and then we could examine for the mass spectra of mesons made of massive quark and antiquarks to assure the GOR relation. We could study the mass relation of the NG boson and the massive scalar modes as expected from the sigma model, which describes well the spontaneous chiral symmetry breaking of QCD. While the modified sigma model might be consistent with our holographic results in the confinement region A, we could not find a simple sigma model that is consistent in both regions A and B.

Finally, we have examined the entanglement entropy to see the role of the dark radiation in the phase transition. In order to make clear the contribution of b_0, the deviation of the entanglement entropy given at $b_0 > 0$ from the one at $b_0 = 0$ is numerically studied. For small $b_0 (< r_0)$, the deviation is small and increases as b_0^4, which is proportional to the energy density of the dark radiation. In the large $b_0 (\gg r_0)$ region, it increases rapidly and is proportional to $b_0^3 \propto T_H^3$. This behavior is the usual thermal behavior expected in the infrared limit of the theory. However, a sharp signature of the phase transition has not been observed.

We would like to mention the relations between our results and those from some four-dimensional effective theory. The Polyakov-Nambu-Jona-Lasinio (PNJL) model has been often used to obtain the QCD phase diagram at finite temperature/chemical potential. In this model, in addition to chiral symmetry breaking/restoration due to the quark-antiquark condensate that was originally developed in the Nambu-Jona-Lasinio model, the confinement-deconfinement phase transition can be taken into account by the Polyakov loop potential. According to the model calculation, T_χ gets higher than T_c. This is a similar result to ours.

In the lattice QCD calculation, however, the result is the opposite. T_χ gets lower than T_c [22]. In [23], the authors tried to reproduce the same result from the PNJL model by including some extra terms, but they did not succeed. As a consequence, even among the four-dimensional approaches, there is no common picture for the properties of QCD phase transition at finite temperature. Physically speaking, in the case with $T_\chi \leq T_c$, massless baryons appear in the temperature regime $T_\chi \leq T \leq T_c$ and they would affect the thermodynamic quantities such as the equation of state.

On the other hand, the chiral phase transition in curved space has been recently discussed [24]. It is suggested that the negative curvature $R < 0$ (the negative cosmological constant) shifts the critical temperature T_χ to the increased one.

ACKNOWLEDGMENTS

The work of M. I. was supported by World Premier International Research Center Initiative WPI, promoted by the Ministry of Education, Culture, Sports, Science and Technology in Japan (MEXT). The work of M. T. is supported in part by the JSPS Grant-in-Aid for Scientific Research, Grant No. 24540280.

[1] J. M. Maldacena, Adv. Theor. Math. Phys. **2**, 231 (1998); The large N limit of superconformal field theories and supergravity, Int. J. Theor. Phys. **38**, 1113 (1999).
[2] S. S. Gubser, I. R. Klebanov, and A. M. Polyakov, Gauge theory correlators from noncritical string theory, Phys. Lett. B **428**, 105 (1998).
[3] E. Witten, Anti–de Sitter space and holography, Adv. Theor. Math. Phys. **2**, 253 (1998).
[4] T. Hirayama, A holographic dual of CFT with flavor on de Sitter space, J. High Energy Phys. 06 (2006) 013.
[5] K. Ghoroku, M. Ishihara, and A. Nakamura, Gauge theory in de Sitter space-time from a holographic model, Phys. Rev. D **74**, 124020 (2006).
[6] K. Ghoroku, M. Ishihara, and A. Nakamura, Flavor quarks in AdS4 and gauge/gravity correspondence, Phys. Rev. D **75**, 046005 (2007).
[7] P. Binetruy, C. Deffayet, U. Ellwanger, and D. Langlois, Brane cosmological evolution in a bulk with cosmological constant, Phys. Lett. B **477**, 285 (2000).
[8] D. Langlois, Brane cosmological perturbations, Phys. Rev. D **62**, 126012 (2000); D. Langlois and L. Sorbo, Bulk gravitons from a cosmological brane, Phys. Rev. D **68**, 084006 (2003).
[9] T. Shiromizu, K. Maeda, and M. Sasaki, The Einstein equation on the 3-brane world, Phys. Rev. D **62**, 024012 (2000).
[10] M. Sasaki, T. Shiromizu, and K. Maeda, Gravity, stability and energy conservation on the Randall-Sundrum brane world, Phys. Rev. D **62**, 024008 (2000); K. Maeda, S. Mizuno, and T. Torii, Effective gravitational equations on brane world with induced gravity, Phys. Rev. D **68**, 024033 (2003).
[11] J. Erdmenger, K. Ghoroku, and R. Meyer, Holographic (de) confinement transitions in cosmological backgrounds, Phys. Rev. D **84**, 026004 (2011).
[12] J. Erdmenger, K. Ghoroku, R. Meyer, and I. Papadimitriou, Holographic cosmological backgrounds, Wilson loop (de) confinement and dilaton singularities, Fortschr. Phys. **60**, 991 (2012).
[13] K. Ghoroku and A. Nakamura, Holographic Friedmann equation and $N = 4$ supersymmetric Yang-Mills theory, Phys. Rev. D **87**, 063507 (2013).
[14] K. Ghoroku, M. Ishihara, and A. Nakamura, AdS5 with two boundaries and holography of $N = 4$ SYM theory, Phys. Rev. D **89**, 066009 (2014).
[15] K. Ghoroku, M. Ishihara, A. Nakamura, and F. Toyota, Glueball instability and thermalization driven by dark radiation, Phys. Rev. D **90**, 126011 (2014).
[16] K. Ghoroku, T. Sakaguchi, N. Uekusa, and M. Yahiro, Flavor quark at high temperature from a holographic model, Phys. Rev. D **71**, 106002 (2005).
[17] T. Sakai and S. Sugimoto, Low energy hadron physics in holographic QCD, Prog. Theor. Phys. **113**, 843 (2005).
[18] M. Gell-Mann, R. J. Oakes, and B. Renner, Behavior of current divergences under $\mathrm{SU}(3) \times \mathrm{SU}(3)$, Phys. Rev. **175**, 2195 (1968).
[19] S. Ryu and T. Takayanagi, Holographic derivation of entanglement entropy from AdS/CFT, Phys. Rev. Lett. **96**, 181602 (2006).
[20] S. Ryu and T. Takayanagi, Aspects of holographic entanglement entropy, J. High Energy Phys. 08 (2006) 045.
[21] B. Swingle and T. Senthil, Universal crossovers between entanglement entropy and thermal entropy, Phys. Rev. B **87**, 045123 (2013).
[22] Y. Aoki, Z. Fodor, S. D. Katz, and K. K. Szabo, The QCD transition temperature: Results with physical masses in the continuum limit, Phys. Lett. B **643**, 46 (2006).
[23] Y. Sakai, K. Kashiwa, H. Kouno, M. Matsuzaki, and M. Yahiro, Determination of QCD phase diagram from the imaginary chemical potential region, Phys. Rev. D **79**, 096001 (2009).
[24] A. Flachi and K. Fukushima, Chiral Mass-Gap in Curved Space, Phys. Rev. Lett. **113**, 091102 (2014).